Molecular Therapy
Nucleic Acids
Original Article

Transplantation of hMSCs Genome Edited with LEF1 Improves Cardio-Protective Effects in Myocardial Infarction

Hyun-Min Cho,[1] Kang-Hoon Lee,[1] Yi-ming Shen,[2] Tae-Jin Shin,[1] Pan-Dong Ryu,[2] Min-Cheol Choi,[3] Kyung-Sun Kang,[4] and Je-Yoel Cho[1]

[1]Department of Biochemistry, BK21 PLUS Program for Creative Veterinary Science Research and Research Institute for Veterinary Science, College of Veterinary Medicine, Seoul National University, Seoul, South Korea; [2]Department of Veterinary Pharmacology, College of Veterinary Medicine, Seoul National University, Seoul, South Korea; [3]Department of Veterinary Radiology, College of Veterinary Medicine, Seoul National University, Seoul, South Korea; [4]Adult Stem Cell Research Center, College of Veterinary Medicine, Seoul National University, Seoul, South Korea

Stem cell-based therapy is one of the most attractive approaches to ischemic heart diseases, such as myocardial infarction (MI). We evaluated the cardio-protective effects of the human umbilical cord blood-derived mesenchymal stem cells (hUCB-MSCs) stably expressing lymphoid enhancer-binding factor 1 (LEF1; LEF1/hUCB-MSCs) in a rat model of MI. LEF1 overexpression in hUCB-MSCs promoted cell-proliferation and anti-apoptotic effects in hypoxic conditions. For the application of its therapeutic effects *in vivo*, the LEF1 gene was introduced into an adeno-associated virus integration site 1 (AAVS1) locus, known as a safe harbor site on chromosome 19 by CRISPR/Cas9-mediated gene integration in hUCB-MSCs. Transplantation of LEF1/hUCB-MSCs onto the infarction region in the rat model significantly improved overall survival. The cardio-protective effect of LEF1/hUCB-MSCs was proven by echocardiogram parameters, including greatly improved left-ventricle ejection fraction (EF) and fractional shortening (FS). Moreover, histology and immunohistochemistry successfully presented reduced MI region and fibrosis by LEF1/hUCB-MSCs. We found that these overall positive effects of LEF1/hUCB-MSCs are attributed by increased proliferation and survival of stem cells in oxidative stress conditions and by the secretion of various growth factors by LEF1. In conclusion, this study suggests that the stem cell-based therapy, conjugated with genome editing of transcription factor LEF1, which promotes cell survival, could be an effective therapeutic strategy for cardiovascular disease.

INTRODUCTION

Myocardial infarction (MI) is the most common coronary heart disease, which in turn, is the leading cause of morbidity and mortality worldwide.[1,2] The main cause of the disease is an obstruction of the coronary artery that leads to a massive loss of cardiomyocytes, resulting in myocardial dysfunction and heart failure.[3] The primary therapy should be the restoration of lost cardiomyocytes, but there is a clear limitation to the regenerative capacity of the adult mammalian heart, meaning that additional therapeutic approaches are mandatory.

Stem cell therapy has received constant attention as a potential strategy for the regeneration of infarcted hearts, and human umbilical cord blood-derived mesenchymal stem cells (hUCB-MSCs) are regarded as a promising candidate for this therapy due to its unique properties, such as multiple lineage potential, lack of teratoma formation, easy expansion, and low immunogenicity.[4] Various trials have treated the injured myocardium using diverse MSC populations, including hUCB-MSCs. Some of these studies showed restoration of damaged cardiomyocytes, enhancement of cardiac function, and to certain degrees, reduced infarct size.[5–7] Although many studies have attempted to utilize hUCB-MSCs and provided positive outcomes in preclinical trials, there are still some hurdles to be surmounted, such as low graft and survival rates in the hostile microenvironment of the infarcted region with its insufficient supply of oxygen and nutrients. Therefore, to enhance hUCB-MSCs' functionality, additional strategies, such as cell patch and genome editing of the hUCB-MSCs, are required to improve cell-survival rate and paracrine effects. There have been a few trials with different target genes that obtained the expected outcomes and addressed these issues. Our recent study reported that hUCB-MSCs overexpressing the vascular endothelial growth factor (VEGF) gene controlled by doxycycline (Dox) induction successfully improved cardiac function via the increase of angiogenesis in MI.[8] VEGF is an angiogenic factor that can promote endothelial cell survival and can be suggested as a therapeutic reagent.[9] Although methods were varied, introduction of islet (ISL) and hepatocyte growth factor (HGF) also enhanced therapeutic effects of stem cells.[10,11] However, there is still room to improve the functionality of hUCB-MSCs via not only endocrine and paracrine growth factors but also autocrine effects. It is ultimately necessary to survey as many therapeutic target genes as possible.

Received 14 August 2019; accepted 8 January 2020;
https://doi.org/10.1016/j.omtn.2020.01.007.

Correspondence: Je-Yoel Cho, DVM, PhD, Professor, Department of Veterinary Biochemistry, College of Veterinary Medicine, Seoul National University, 1 Gwanak-ro, Gwanak-gu, Seoul, South Korea.
E-mail: jeycho@snu.ac.kr

We indeed focused on the activation of canonical wingless/integrase-1 (Wnt) signaling pathways that have been known to contribute to mouse embryonic stem cell (ESC) self-renewal and help maintain the undifferentiated status of ESCs through modulation of Oct4 and Nanog.[12–14] Lymphoid enhancer-binding factor-1 (LEF1), a 48-kD nuclear protein, is a crucial transcription factor for proliferation and survival of B and T cells.[15,16] The involvement of LEF1 in canonical Wnt signaling pathways has been studied, and activation of the pathways via the overexpression of LEF1 has been shown to contribute to mouse ESC self-renewal.[13] Furthermore, it has also been reported that the gene regulates the follicle morphogenesis and proliferation of neural progenitor cells.[17,18]

Recent studies have focused on the functions of LEF1 related to stem cells and cardiogenesis. High expression of LEF1 between the mesoderm and cardiac progenitor cell stage has been identified in various studies, and it has been suggested that the gene plays an important role between these stages.[19,20] Moreover, direct and temporal contribution of LEF1 in mouse heart maturation has also been reported. It has been demonstrated that the gene is mainly expressed in MSCs in the valvular region during the murine heart development,[21] but its function in mouse and human MSCs (hMSCs) needs additional study. Despite this positive potential in cell proliferation, survival, and cardiac differentiation, the cardio-protective effects from MI in stem cell therapy have not been demonstrated yet.

In parallel, diverse gene introduction systems, such as viruses, zinc-finger nucleases, transcription activator-like effector nucleases (TALENs), and CRISPR and CRISPR-associated 9 (Cas9), have been developed.[22–25] Since 2012, when the CRISPR system was initially demonstrated, it has been improved to reduce off-target mutations[25] and has been widely adopted as the simplest and most efficient gene-integration systems in various cells and organisms, including human, rat, and mouse.[26–28]

Taken together, the objective of this study is to examine the therapeutic efficacy of the hUCB-MSCs stably expressing the LEF1 by CRISPR/CAS9-mediated gene integration (LEF1/hUCB-MSCs) in MI. We first investigated autocrine effects of overexpressing LEF1 in hUCB-MSCs on cell proliferation and survival of hUCB-MSCs in both normal and oxidative stress conditions and then survival-promoting effects of the cells in the MI region *in vivo*. Moreover, paracrine effects via stimulation of growth factor and cytokine secretion by LEF1 were also analyzed to explain the recovery of cardiac function in the MI animal model by LEF1.

RESULTS

LEF1 Promotes hUCB-MSC Proliferation

To find the target gene for hUCB-MSC therapy, we examined multiple transcriptome analyses from 4 different studies that were associated with cardiomyocyte differentiation from pluripotent cells, since the genes that exhibit cell-specific expression from mesoderm to cardiac progenitor cell stage promote self-renewal to maintain the stage or differentiation to cardiac progenitor cells.[29–31] We focused on genes that are enriched in these stages. From 8 different analyses, we first examined the 100 most strongly upregulated genes in these stages in comparison to human pluripotent stem cells and then listed them individually in supplemental data (Table S1). From these gene lists, the 11 genes that were commonly enriched in 5 or more analyses were selected (Figure S1A). Among these, 36% (4 out of 11) of the genes are known to function in cardiac differentiation, e.g., *PLXNA2*, *TBX3*, and *BMP4*, and in MSC proliferation, e.g., *LIX1*, and were excluded from further target selection, finally leaving only 7 target genes.

The 7 target genes selected from the *in silico* literature surveys were subjected to conventional PCR (Figure S1B) and qRT-PCR to examine the gene expression in hUCB-MSCs and expression patterns during the cardiomyocyte differentiation. Various patterns were observed (Figure S2), but the aim of this study was to enhance the protection efficacy of hUCB-MSCs by insertion of target genes, so we focused on the genes that maintained a constant low expression (*LEF1*, *ZEB2*). However, the effects of LEF1 on cell proliferation, as well as the direct and temporal contributions to heart development, have been reported.[13,21,32] Consequently, all additional studies proceeded with LEF1 (Figures 1A and 1B). Since low-proliferative capacity is one of the limits in the use of differentiated stem cells,[33] we first examined if introducing LEF1 would enhance hUCB-MSC proliferation. The hUCB-MSCs transfected with LEF1 showed significantly increased numbers of cells, 72 h after incubation, without any aberrant changes in morphology (Figures 1C and 1D). The activation of canonical Wnt/β-catenin signaling by LEF1 transfection was confirmed by RT-PCR of β-catenin (CTNNB1) and c-Myc, as well as LEF1 itself. LEF1 significantly increased the expression of CTNNB1 and c-Myc. Cyclin D1 expression was also dramatically increased, representing stimulated cell cycles by LEF1 (Figures 1E and 1F). This result was confirmed in protein levels, as western blot and densitometry analysis clearly showed that Wnt/β-catenin signaling and cyclin D1 were upregulated by LEF1 (Figures 1G and 1H). We then presented the evidence for the proliferative fate of hUCB-MSCs enhanced in LEF1 transfection. Cell-cycle analysis using propidium iodide (PI) staining, combined with an automated fluorescence cell counter, showed cell fates shifted up from G0/G1 to S phases in the LEF1-transfected hUCB-MSC population. Approximately 40% cell-cycle enhancement was observed within the hUCB-MSCs transfected with LEF1 (Figures 1I and 1J).

LEF1 Prevents hUCB-MSCs from Hydrogen Peroxide-Induced Apoptosis

A major issue in stem cell therapy for ischemic heart diseases, including MI, is the low survival of transplanted cells in the ischemic region. It is reported that most hMSCs implanted onto ischemic hearts died within 4 days after transplantation.[34] Therefore, we examined the protective function of LEF1 from the hydrogen peroxide-induced cell death of hUCB-MSCs *in vitro*. Apoptosis was induced by 500 μM H_2O_2 treatment for 48 h in hUCB-MSCs, whereas hUCB-MSCs expressing LEF1 still survived at a significantly higher number of cells (Figure 2A). Slightly more cells were counted in

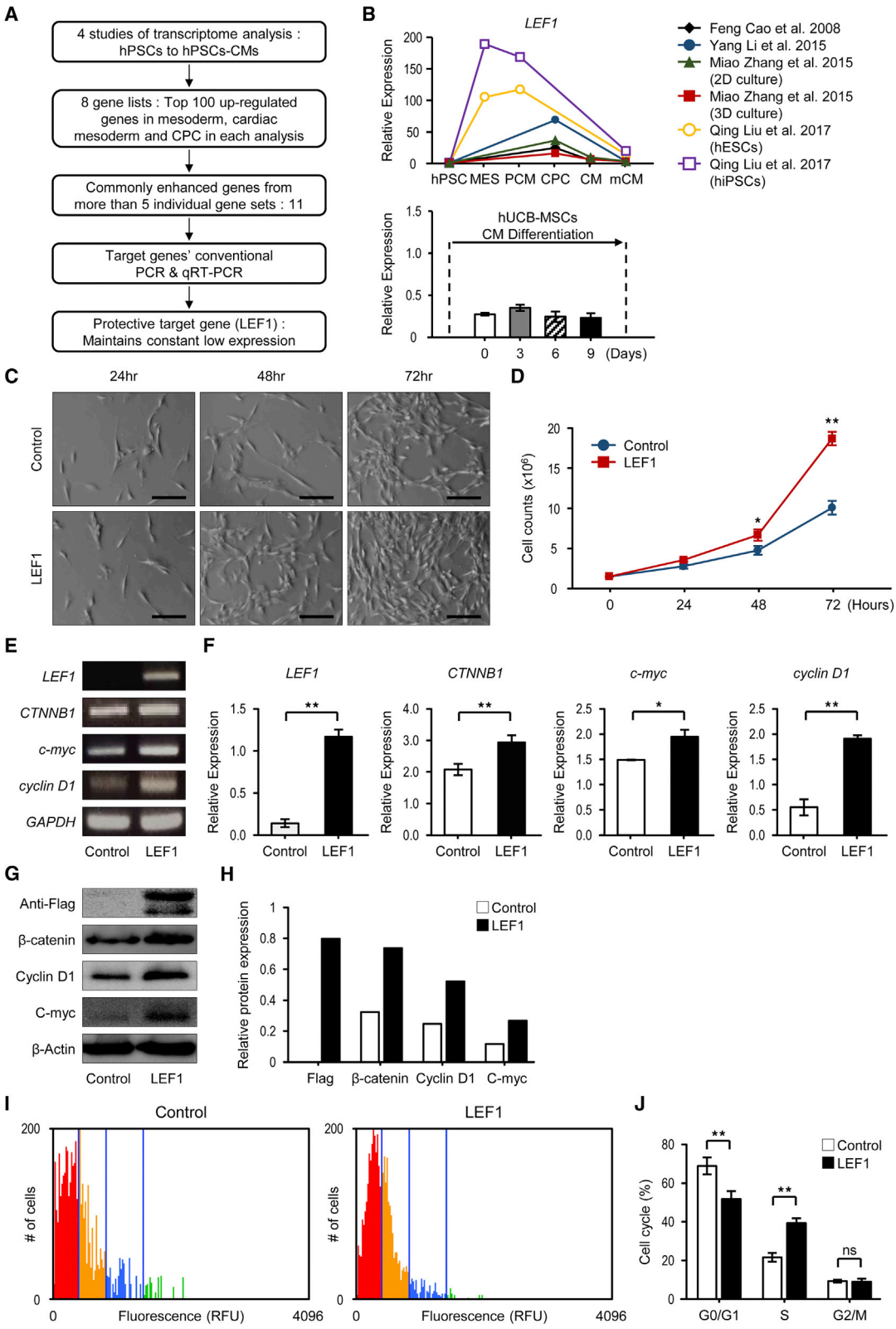

(legend on next page)

LEF1-transfected hUCB-MSCs than in the control hUCB-MSCs under normal conditions. Yet, the number of cells remained drastically higher in the LEF1-expressing hUCB-MSC group (80% survival) than the control hUCB-MSC group (30% survival) under severe oxidative stress conditions induced by H_2O_2 (Figure 2B). Western blot analysis for Bax and Bcl-2 proteins revealed that LEF1 blocked proapoptotic Bax but induced anti-apoptotic Bcl-1, even without oxidative stress, thus presenting a reduced level of Bax but an increased level of Bcl-2 in both normal and severe oxidative stress conditions (Figures 2C–2E). These results demonstrate that the cells had a protective effect upon H_2O_2 treatment. We next demonstrated that LEF1 could protect hUCB-MSCs from apoptosis under severe oxidative stress using flow cytometry with Annexin V/PI labeling. As shown in Figures 2F and 2G, a drastic increase in the apoptotic cells was observed in control hUCB-MSCs upon H_2O_2 treatment (~25%). However, a remarkable reduction in the apoptotic cell ratio was shown in LEF1-transfected hUCB-MSCs under both normal (~4%) and oxidative stress conditions (~10%). Altogether, these results indicate that the LEF1 plays an important role in anti-apoptosis of hUCB-MSCs under oxidative stress.

LEF1/hUCB-MSC Transplantation Improves Cardiac Dysfunction after Myocardial Infarction

A number of studies have demonstrated that stem cell therapy is effective in myocardial regeneration via enhancement of angiogenesis in the region of MI.[33] Various types of stem cells, different treatments or gene editing, and transplantation methods have been developed and tested to improve therapeutic efficacy.[35] In the present study, we first constructed LEF1/hUCB-MSCs that steadily express LEF1 using the CRISPR/Cas9 system, followed by homologous recombination on the AAVS1 genomic safe harbor site (Figure 3A). Successful integration of LEF1 on AAVS1 was confirmed by genomic PCR spanning from LEF1 to the AAVS1 site (Figures 3B and 3C). LEF1 protein was stably expressed by LEF1/hUCB-MSCs until 14 days after transfection (Figure 3D). To determine the cardioprotective potential of LEF1/hUCB-MSCs in ischemic heart disease, we conducted an experiment using transplantation of LEF1/hUCB-MSCs and control hUCB-MSCs in a post-MI rat model. This experiment included a group of sham rats (surgery without MI) and MI rats (nontreat with MI) as controls (Figure 3E). The cell transplantation of each group was administered as a cell patch using the UpCell system (Figure 3F).

A total of 20 rats, 5 rats in each group, was initially designed and subjected to MI surgery. The rats were randomized to the following groups: operation + non-MI, MI + nontreat, MI + hUCB-MSCs, MI + LEF1/hUCB-MSCs. Each cell sheet was transplanted 30 min after visual inspection of the infarction. However, 6 out of 11 rats with MI died within 2 weeks after the operation (45.5% survival). Three out of 8 (62.5% survival) died in the MI + hUCB-MSC group and 1 out of 6 in the MI + LEF1/hUCB-MSC group (83.3% survival) (Figure 3G).

To measure the combined therapy in MI, we performed echocardiography at 1 week and 4 weeks after MI surgery (Figure 4A). A successful induction of MI in the rat model was confirmed by echocardiography showing drastic reduction of left-ventricular ejection fraction (EF) (sham: 89.01 ± 2.56% versus MI: 36.33 ± 5.11%) and fraction shortening (FS) (sham: 60.48 ± 3.82% versus MI: 16.24 ± 1.41%) when comparing the sham and MI group at 1 week postsurgery (Figures 4B and 4C). Damage of the heart muscle was also measured by an increase of the left ventricle (LV) inner diameter at diastole (LVIDd) (sham: 4.33 ± 0.41 mm versus MI: 8.77 ± 0.27 mm) and LV inner diameter at systole (LVIDs) (sham: 2.26 ± 0.33 mm versus MI: 7.60 ± 0.41 mm) (Figures 4D and 4E). To evaluate functional improvement of hUCB-MSCs and LEF1 overexpression in hUCB-MSCs on the MI, we also measured these 4 values at 4 weeks postsurgery (Figures 4B–4E). The MI + hUCB-MSC group tended to have some protective effects when compared with MI, but there was no significant difference between the values taken 1 and 4 weeks postsurgery: EF (43.56 ± 3.62%), FS (21.6 ± 1.88%), LVIDd (8.68 ± 0.37 mm), and LVIDs (7.64 ± 0.18 mm). Of note, in the comparison among the three MI groups (MI alone, MI + hUCB-MSCs, and MI + LEF1/hUCB-MSCs), LEF1 expressing hUCB-MSCs significantly improved in all 4 functional values in 4 weeks: EF (63.53 ± 4.34%), FS (37.11 ± 2.78%), LVIDd (6.29 ± 0.19 mm), and LVIDs (4.72 ± 0.34 mm). These results demonstrate the protective effects of LEF1/hUCB-MSCs in MI when compared with the MI-alone group and with the MI + hUCB-MSC group as well: EF (29.18 ± 5.13%), FS (12.36 ± 2.21%), LVIDd (9.30 ± 0.31 mm), and LVIDs (7.71 ± 0.42 mm).

LEF1/hUCB-MSCs Show Reduced MI Size and Fibrosis and Protect the Left-Ventricular Wall from Thinning

Transplantation of LEF1/hUCB-MSCs reduced MI size and fibrosis and protected the left-ventricular wall from thinning (Figure 5). The improvement of cardiac function was observed from a histological analysis. Masson's trichrome staining on the rat heart, 4 weeks after sham surgery, presented heart muscle in red (Sham in Figure 5A). The other three hearts with induced MI produced different ranges of regions stained with blue, which represents fibrosis in the LV. A very

Figure 1. Selection Process of Therapeutic Target Gene LEF1 and Cell-Proliferation Effects of LEF1 in hUCB-MSCs

(A) Schematic depiction of the overall workflow. (B) Comparison of LEF1 gene expression with *in silico* literature surveys and qRT-PCR data. (C) Representative images from phase-contrast microscopy at 24, 48, and 72 h after LEF1 transfection of hUCB-MSCs. Scale bars, 100 μm. Control (Ctrl): no DNA; LEF1: LEF1:pDC3.1. (D) hUCB-MSCs (1.5×10^5 cells), treated with no DNA or LEF1:pDC3.1, were seeded, and the increased number of cells was counted at the 24-, 48-, and 72-h time points. *$p < 0.05$ and **$p < 0.01$. (E) Conventional PCR for the Wnt pathway and cell-cycle-related genes. (F) Significant difference in gene-expression levels was confirmed by real-time PCR. Relative expression to GAPDH was calculated by the ΔΔ CT method. **$p < 0.01$. (G) Western blot analysis confirmed the increased expression in protein level under LEF1 overexpression. (H) Densitometry showed relative protein expression to β-actin level. (I) Cell-cycle analysis was performed by automated fluorescence cell counting in hUCB-MSCs differentially treated with no DNA or LEF1:pDC3.1. Colors indicate different stages; red: G0/G1 phase; yellow: S phase; blue: G2/M phase. (J) The histogram for the cell-cycle distribution after transfection of LEF1 and scrambled control DNA. **$p < 0.01$ compared to control.

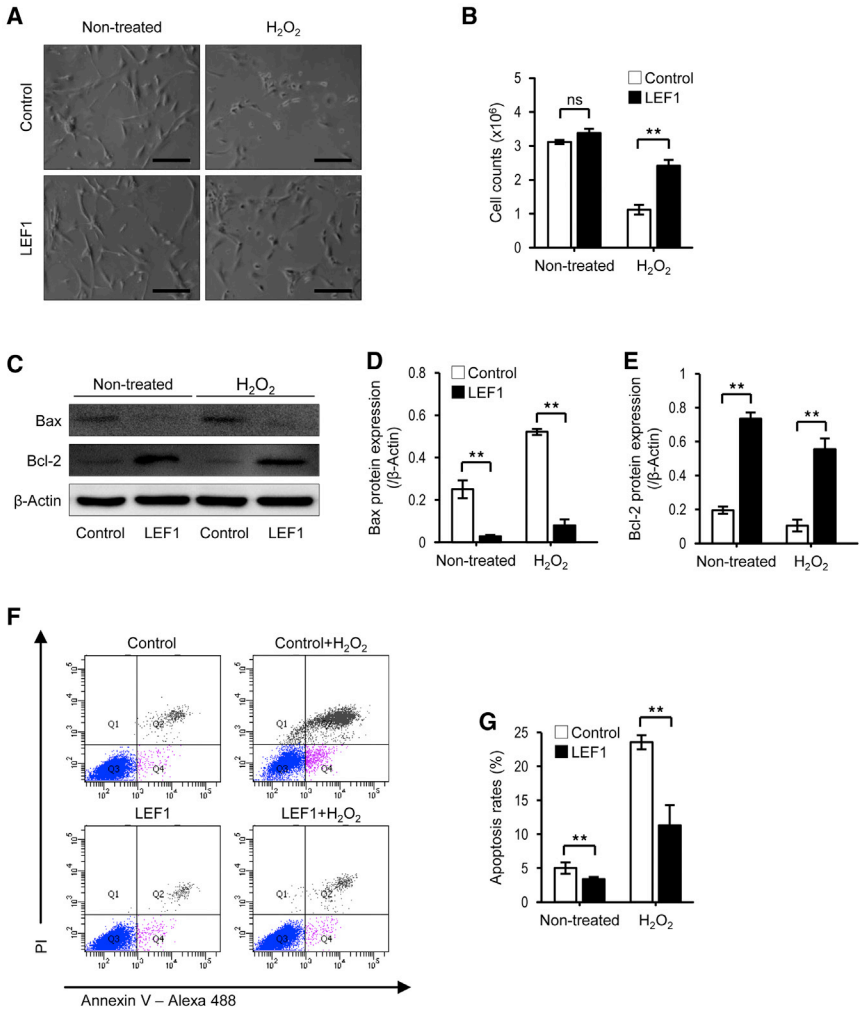

Figure 2. LEF1 Overexpression Protects hUCB-MSCs from Oxidative Stress-Induced Apoptosis

(A) Microscopy demonstrated that oxidative stress-caused cell death was attenuated by LEF1 overexpression. Scale bars, 100 μm. (B) Quantification of reduced cell death in LEF1 overexpression under oxidative stress condition. **$p < 0.01$. (C) Drastic increase in Bcl-2 and decrease in Bax expression in LEF1-overexpressing hUCB-MSCs were observed by western blot. (D and E) Image analysis confirmed the significant changes of Bax (D) and Bcl-2 (E) expression in LEF1-overexpressing hUCB-MSCs. (F) Fluorescence-activated cell sorting (FACS) analysis using PI and Annexin V successfully presented increased apoptotic cell populations (Q2) under H_2O_2 treatment in hUCB-MSCs (top right), but less cells were dead in LEF1-expressing hUCB-MSCs (bottom right). (G) Reduced apoptosis triggered by H_2O_2 in LEF1 transfection. **$p < 0.01$.

thin, blue-stained wall fiber was detected in the MI-induced control model. No live heart muscle was stained in the MI region. Instead, a little thicker LV was noted in the hUCB-MSC-treated MI group, but large fibrosis was still stained. Some live heart cells stained in red could be seen in the region of fibrosis. This may indicate that hUCB-MSC itself has a minor protective effect (MI + hUCB-MSCs in Figure 5A). In particular though, a clear improvement in the anti-fibrosis effect was detected in the group treated with LEF1/hUCB-MSCs (MI + LEF/hUCB-MSCs in Figure 5A). The region of fibrosis stained blue was greatly reduced and the number of heart muscle cells remaining (stained with red) in the fibrotic region were more readily observed in the magnified image (Figure 5A). For the quantitation of efficacy in cardiac function, three factors, MI-size, fibrosis, and wall thickness, were measured by analyzing the stained areas. MI-size and fibrosis were dramatically decreased in the LEF1/hUCB-MSC group when compared with both the MI and MI + hUCB-MSC groups (Figures 5B and 5C). Furthermore, the decrease of LV wall thickness resulting from MI was significantly protected from the LEF1/hUCB-MSC group, whereas the LV wall thickness tends to appear drastically reduced in the hUCB-MSC group, which was not significantly different from the MI group (Figure 5D). These results suggest that LEF1 abundantly expressed in hUCB-MSCs not only has an autocrine effect (enhancing the survival of hUCB-MSCs) but also somehow has paracrine effects, possibly via growth factors and cytokines, which can protect and regenerate damaged rat heart cells in the region of MI.

LEF1 Expression in hUCB-MSCs Helps to Prolong Survival of Implanted Stem Cells in MI

LEF1 expression was confirmed by immunohistochemical staining in MI-induced rat heart tissues. Fibrous heart structure was found in the MI-only group with few cells stained with methyl green (MI in Figure 6A). There were some cells that survived in the patch of hUCB-MSCs, but no LEF1 expression was detected in the MI + hUCB-MSC group. LEF1 expression was stained only in the tissues from the cell patch of LEF1/hUCB-MSCs attached on the MI region (MI + LEF1/hUCB-MSCs in Figure 6A). This suggests that there was no endogenous expression of LEF1 in the patched hUCB-MSCs. In addition, substantially more cells were counted in the LEF1/hUCB-MSC group than the hUCB-MSC group, 4 weeks after surgery. This might contribute to the thicker LV in the MI region with LEF1/hUCB-MSCs. Quantification of the LEF1 immunohistochemistry (IHC) data successfully displayed prolonged survival of LEF1/hUCB-MSCs (Figure 6B). To distinguish implanted human stem cells from rat heart cells, IHC with anti-lamin A + C antibody was performed in the MI region. We took a picture from the edge of the MI region to include rat heart cells as a control. No lamin A + C-positive cells were detected from rat heart cells in the MI group (Figure 6C). Only a thin layer of human cells was stained with lamin A + C-positive cells in the hUCB-MSC

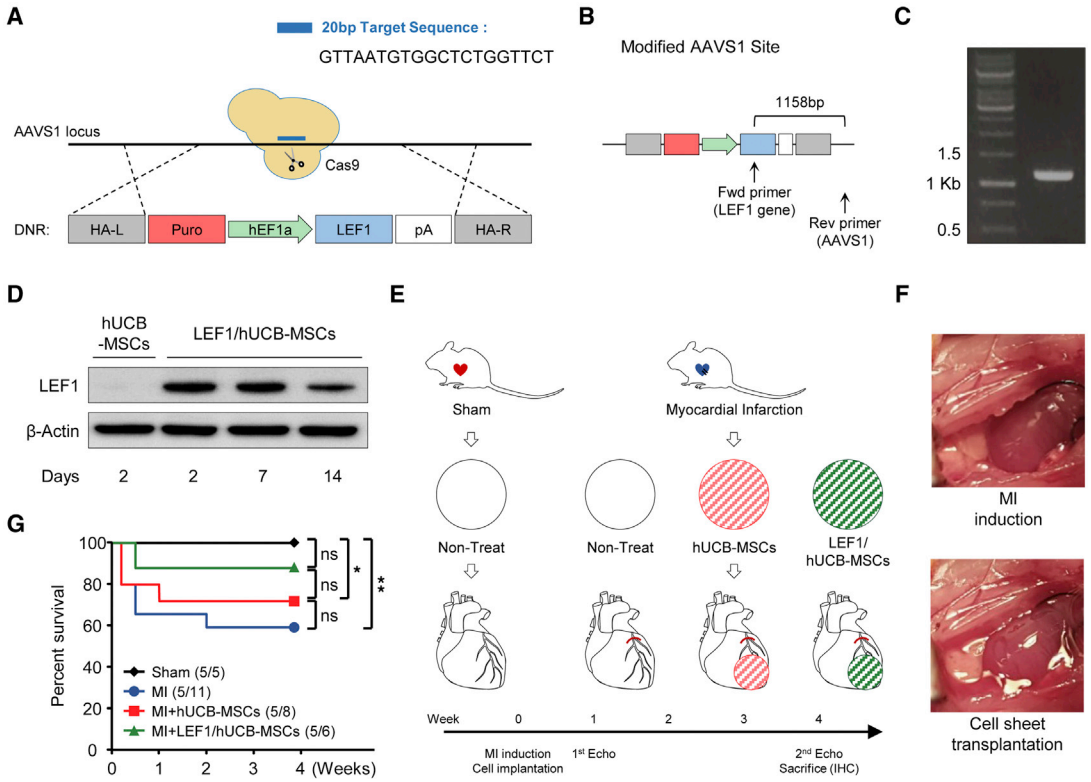

Figure 3. Experimental Strategy of the Therapeutic hUCB-MSC Transplantation System

(A) Schematic diagram of the LEF1 gene-integration procedure by CRISPR/Cas9-mediated knockin to the AAVS1 site of hUCB-MSCs. 20-nt-length single-guide RNA (sgRNA) target sequence on the AAVS1 locus; LEF1 introduction cassette flanked by homologous arm (HA) left (HA-L) and right (HA-R) were indicated. (B) The architecture of donor DNA in the AAVS1 locus. Arrows: primers designed for the detection of successful homologous recombination. (C) Confirmation of the correct integration of the LEF1 cassette into the AAVS1 locus using PCR (1,158 expected size). (D) Western blot analysis showing stable expression of LEF1 protein from LEF1/hUCB-MSCs for 2 weeks. (E) Schematic illustration of the therapeutic procedure with cell-sheet transplantation of hUCB-MSCs and LEF1/hUCB-MSCs in an MI model. Of note, the cell-sheet transplantation was performed with induction surgery of MI on day 0, and echocardiography measurements were performed prior to MI surgery, as well as 1 week and 4 weeks after transplantation. The four groups are Sham: surgery without MI; MI: MI alone; MI + hUCB-MSCs: MI treated with hUCB-MSCs; and MI + LEF1/hUCB-MSCs: MI treated with LEF1/hUCB-MSCs. (F) Representative images depicting before and after MI induction and stem cell transplantation using the UpCell system. (G) Survival curves of the experimental groups. The survival rate was significantly enhanced in the LEF1/hUCB-MSC group (n = 5–11). *$p < 0.05$; **$p < 0.01$; ns, not significant.

groups, whereas a large number of lamin A + C-positive, implanted human stem cells were detected in the MI + LEF1/hUCB-MSC groups. Strikingly, rat heart myocardium still remained thicker at 4 weeks after MI induction following LEF1/hUCB-MSC treatment (Figure 6D). These results suggest that LEF1 expression in hUCB-MSCs has positive effects, not only on the survival of stem cells but also on protecting rat myocardial cells from MI via paracrine effects.

LEF1 Expression in hUCB-MSCs Triggers the Production of Various Growth Factors that Protect the Heart and Promote VEGF Production and Angiogenesis in MI

Growth factors and cytokines, such as VEGF, insulin-like growth factor (IGF), HGF, interleukin-1β (IL-1β), and IL-6, have been investigated as therapeutic targets in various cell types and diseases.[8,36–38] Recently, these molecules, secreted by MSCs, have been examined in repair and regeneration therapy.[35] We thus investigated the paracrine effect of LEF1/hUCB-MSCs via enhanced secretion of growth factors and cytokines. Expression levels of three growth factors (HGF, IGF, and VEGF) and the cytokine (IL-8) were compared between control hUCB-MSCs and LEF1/hUCB-MSCs. As expected, HGF, IGF, VEGF, and IL-8 were increased in LEF1/hUCB-MSCs (Figure 7A). Quantitative RT-PCR showed an approximate 2-fold increase in the expression of VEGF, IL-8, and IGF in LEF1/hUCB-MSCs (Figure 7B). VEGF protein expression was confirmed by IHC staining (Figure 7C). Rat heart at the edge of the MI region was faintly stained due to crossreactivity of the VEGF antibody between human and rat. A strong VEGF signal was detected in the surrounding regions of LEF1/hUCB-MSCs (Figure 7D). Since VEGF is known to assist in angiogenesis, we measured the vascular genesis in the MI regions of the MI, MI + hUCB-MSC, and MI + LEF1/hUCB-MSC groups using von Willebrand factor (vWF) IHC staining. Of these, the LEF1/hUCB-MSC groups showed higher vessel density than the other two groups (Figures 7E and 7F). These results

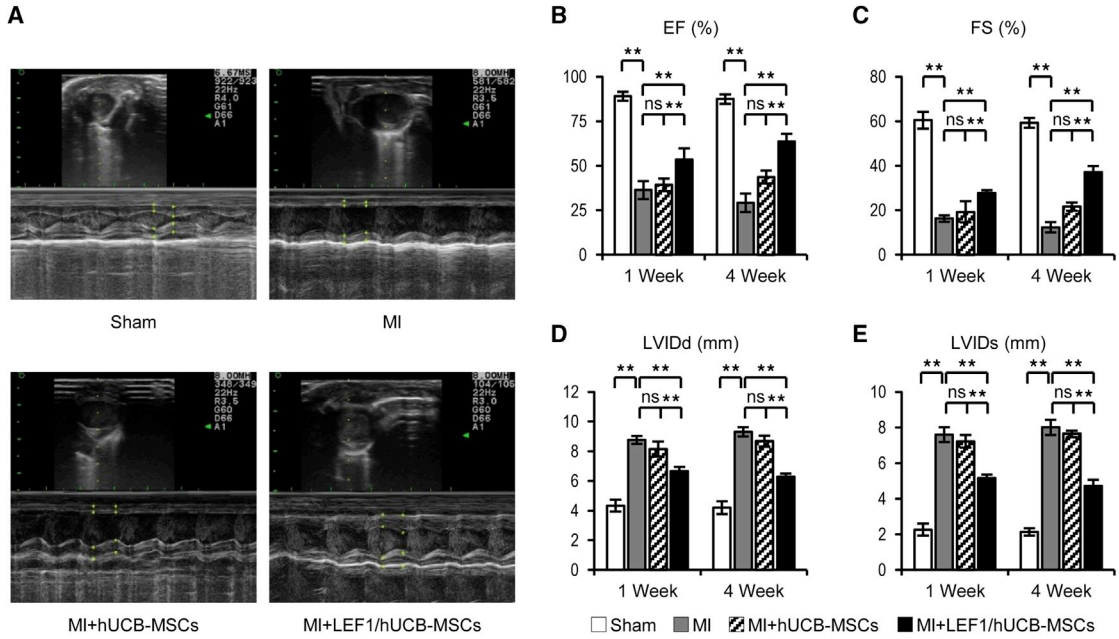

Figure 4. Transplantation of LEF1/hUCB-MSCs Recovered Cardiac Function in MI Rat

(A) Representative images of echocardiography showed successively improved cardiac function in MI, MI + hUCB-MSCs, and MI + LEF1/hUCB-MSCs at 4 weeks postsurgery. (B–E) Four values representing cardiac function (EF in B; FS in C; LVIDd in D; and LVIDs in E) were measured and compared in histograms. Significant improvements were detected in all MI + LEF1/hUCB-MSC groups.*$p < 0.05$, **$p < 0.01$; ns, not significant. Error bar: standard error. White bars, Sham; gray bars, MI; striped bars, MI + hUCB-MSCs; black bars, MI + LEF1/UCB-MSCs.

determined that LEF1 integration in hUCB-MSCs triggers the expression of diverse growth factors and enhances vessel formation, resulting in protective effects on myocardial cells in the rat MI model.

DISCUSSION

Stem cell-based therapies have emerged as a promising treatment for heart regeneration after infarction.[33] Among them, hUCB-MSCs have been recognized as good candidates, due to trophic activities, such as multiple lineage potential, lack of teratoma formation, easy expansion, and low immunogenicity.[39] In cardiovascular disease, MSC-based therapies have been attempted in a lot of preclinical research and have shown sufficient potential. However, the low cell-survival rates and the engraftment failure of implanted cells in the infarcted region are the main obstacles in this field that still remain. Therefore, enhancement of stem cell proliferation and its survival under the harsh conditions of the ischemic area is necessary to utilize MSCs for clinical application.

In the current study, we thus focused on enhancing stem cell activities in cell proliferation and its survival in the harsh conditions of the ischemic region. LEF1 has been known to play a role in regulating cell proliferation via Wnt/β-catenin signaling.[12,32,40] Huang and Qin[13] recently reported that LEF1 plays a crucial role in sustaining self-renewal in mouse ESCs as well. Therefore, we investigated the effects of LEF1 expression in hUCB-MSCs in normal and harsh conditions, such as oxidative stress *in vitro*. Introduction of LEF1 to hUCB-MSCs resulted in the overexpression of LEF1-stimulated stem cells' cell cycle and proliferation via the canonical Wnt pathway in normal conditions (Figure 1). In addition, the understanding of the cell response to oxidative stress *in vitro* is important because the cells' microenvironment after implantation is hypoxic, which can lead to apoptosis.[41] This study clearly showed that LEF1 expression protected hUCB-MSCs from oxidative stress conditions by increasing Bcl-2 expression. This was confirmed through flow cytometry, showing a reduced number of apoptotic cells induced by H_2O_2 (Figure 2).

We then generated therapeutic hUCB-MSCs that stably express LEF1 through CRISPR/Cas9-mediated genome editing (LEF1/hUCB-MSCs) in order to examine whether the induction of the LEF1 gene in hUCB-MSCs affects the cell engraftment, survival, and tolerance in hypoxic conditions. The CRISPR/Cas9 gene integration system was employed on the AAVS1 locus to overcome side effects, such as tumorigenesis, or unpredictable integration of the transgene, which could be induced by the viral approach.[28] Steady expression of LEF1 was detected until 2 weeks in LEF1/hUCB-MSCs. As expected from the *in vitro* study, the LEF1/hUCB-MSC group showed strong, positive effects in the *in vivo* MI model. Echocardiography and histological staining analysis clearly showed evidence that LEF1/hUCB-MSCs have a protective effect in the MI region. EF, FS, LVIDd, and LVIDs, which represent left-ventricular cardiac functions, were greatly improved in LEF1/hUCB-MSCs compared with MI alone and hUCB-MSC treatment.

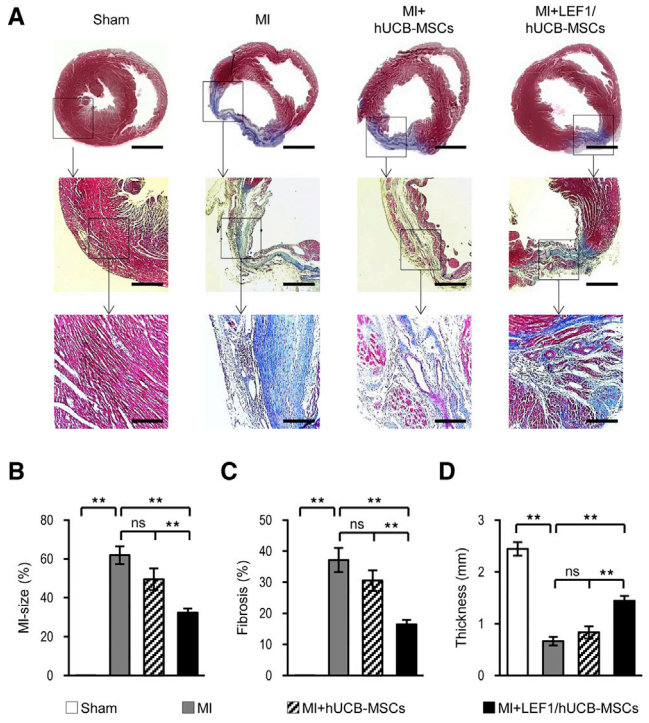

Figure 5. The LEF1/hUCB-MSC Transplantation Greatly Reduced MI Size and Fibrosis and Restored the LV Wall Thickness

(A) Masson's trichrome staining showed MI regions at 4 weeks after surgery. Scale bars: top row, 1 mm; middle row, 400 μm; bottom row, 200 μm. The red-stained region means the viable myocardium, and the blue-stained region means the fibrotic area. The large, fibrous region stained in blue is found in MI alone compared to MI + hUCB-MSCs and MI + LEF1/hUCB-MSCs. Serial magnification distinctively presented damaged heart in MI and enhanced heart-protective efficacy of MI + LEF1/hUCB-MSCs. (B–D) Quantification of infarct size (B), fibrosis region (C), and the wall thickness (D) of LV in each group (n = 5). *p < 0.05, **p < 0.01; ns, not significant.

In addition, the protective effect of LEF1/hUCB-MSCs was measured by MI-size, fibrosis, and wall thickness using Masson's trichrome staining. MI and fibrosis were formed approximately 52% less in LEF1/hUCB-MSCs compared with the MI control group. This is a huge improvement compared with the hUCB-MSC group, showing only a 21% reduction. Furthermore, wall-thickness loss in MI was suppressed by LEF1/hUCB-MSCs, whereas it was not significantly different between MI alone and the MI + hUCB-MSC group. Most cardiac muscle cells were replaced by fibrosis in MI alone, but heart muscle structure was still retained in the MI region treated with LEF1/hUCB-MSCs. This result may suggest two major mechanisms to explain these enhanced therapeutic effects. One is a paracrine effect, and the other one is direct transdifferentiation. After transplantation, the engrafted MSCs could secrete the therapeutic factors that regenerate the damaged cardiac tissue and cause neovascularization via paracrine effects and also prevent the cell loss of cardiomyocytes by direct transdifferentiation or inhibition of fibrosis. However, according to previous studies, there is little evidence that the induction of the LEF1 gene in stem cells directly affected the differentiation of cardiomyocytes or the decrease of fibrosis. In contrast, it has been reported that LEF1 expression secretes many therapeutic factors associated with cell cycling, proliferation, and survival.[12,13,32,42] This mechanism that enhances positive effects in cell-cycle, proliferation, and cell survival under oxidative stress was confirmed by this *in vitro* study (Figures 1 and 2). We also tested paracrine effects of LEF1 expression in hUCB-MSCs. As we showed in Figure 7, increased VEGF and IL-8 expressions were detected in LEF1/hUCB-MSCs *in vitro* and were confirmed by IHC in a rat MI model with transplanted LEF1/hUCB-MSCs. These results indicated that LEF1/hUCB-MSCs enhanced the secretion of various growth factors associated with microenvironmental neovascularization, proliferation, and immune responses, resulting in protective effects on hearts damaged by MI.

Although we presented several positive aspects of genome editing to lead LEF1 expression in hUCB-MSCs, there are also several studies regarding the aberration of LEF1 gene expression in various cases of tumorigenesis and cancer cell proliferation, migration, and invasion.[43,44] Particularly, LEF1 expression has been reported in cancer cell types, such as some leukemias, lymphoma, squamous cell carcinoma, and colorectal cancer.[45,46] Lack of teratoma formation has been known in MSCs; however, the tumorigenic effect of LEF1 in hUCB-MSCs needs be tested in regard to long-term expression and survival.

In conclusion, we provide the evidence that LEF1 promotes hUCB-MSC proliferation and attenuates the apoptosis from oxidative stress. The hUCB-MSCs in which the LEF1 gene was integrated by the CRISPR/Cas9 system displayed enhanced cell survival and improved cardio-protective effects in an animal model of MI. These results suggest that the introduction of LEF1 could be a novel strategy in stem cell therapy after MI.

MATERIALS AND METHODS

Isolation and Culture of hUCB-MSCs

hUCB-MSCs were isolated, as previously described,[47] and by following the procedure approved by the Borame Hospital institutional review board (IRB) and Seoul National University (IRB No. 0603/001-002-07C1). In brief, UCB samples were harvested from term and preterm deliveries at the time of birth with the mother's informed consent (Seoul City Borame Hospital Cord Blood Bank). Separation of the MSCs from UCB was performed using Ficoll-Paque PLUS (Amersham Bioscience, Uppsala, Sweden). The cells were suspended in DMEM (Gibco, Grand Island, NY, USA) with 20% fetal bovine serum (FBS; Gibco), 100 IU/mL penicillin, 100 mg/mL streptomycin, 2 mM L-glutamine, and 1 mM sodium pyruvate. After 24 h, the cells were washed twice in PBS and cultured in DMEM with 10% FBS.

Transfection and Cell-Proliferation Assays

To introduce the expression vector, transfection was performed using Lipofectamine 3000 by following the manufacturer's manual (Thermo Fisher Scientific, Waltham, MA, USA). The hUCB-MSCs and LEF1-introduced hUCB-MSCs were subjected to a

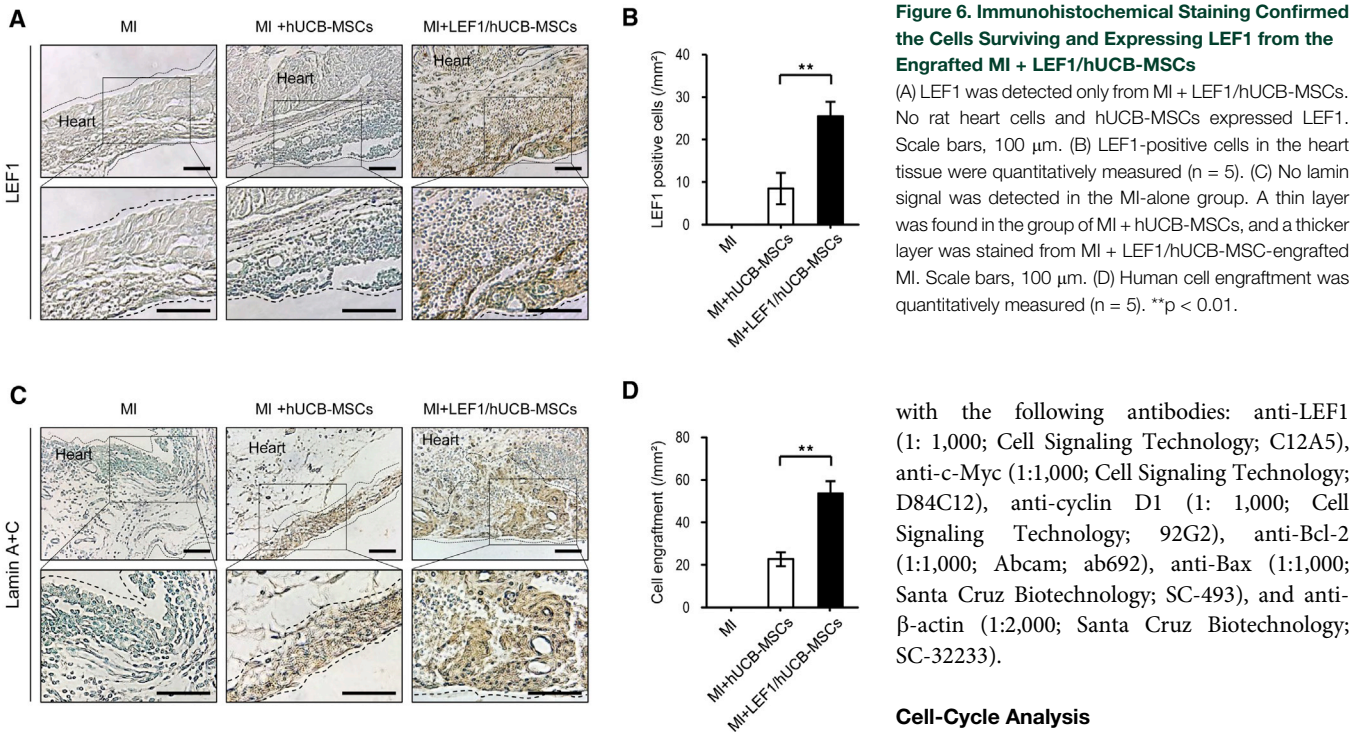

Figure 6. Immunohistochemical Staining Confirmed the Cells Surviving and Expressing LEF1 from the Engrafted MI + LEF1/hUCB-MSCs

(A) LEF1 was detected only from MI + LEF1/hUCB-MSCs. No rat heart cells and hUCB-MSCs expressed LEF1. Scale bars, 100 μm. (B) LEF1-positive cells in the heart tissue were quantitatively measured (n = 5). (C) No lamin signal was detected in the MI-alone group. A thin layer was found in the group of MI + hUCB-MSCs, and a thicker layer was stained from MI + LEF1/hUCB-MSC-engrafted MI. Scale bars, 100 μm. (D) Human cell engraftment was quantitatively measured (n = 5). **p < 0.01.

cell-proliferation assay. In brief, 150,000 cells were seeded in 60 mm plates on day 0 and counted after 24 h, 48 h, and 72 h by an automated cell counter (Arthur; NanoEnTek, Seoul, Korea). Experiments were run in triplicate.

RNA Isolation and cDNA Synthesis

The total RNA was extracted by using the TRIzol reagent (Invitrogen, Carlsbad, USA), and the quality was measured by the ratio of 260/280 using the Nanodrop Epoch Microplate Spectrophotometer (BioTek Instruments, VT, USA). Reverse transcription was performed on 2 μg of RNA using the Omniscript RT kit, following the manufacturer's guideline (QIAGEN), TRIzol reagent (Invitrogen, Carlsbad, USA).

Conventional and Real-Time PCR Analyses

Conventional PCR was performed on 1 μL of cDNA using GoTaq polymerase in the following conditions: denaturation at 95°C for 2 min, 35 cycles of 95°C for 30 s, 60°C for 30 s, and 72°C for 30 s, followed by final extension at 72°C for 5 min. Real-time PCR was performed in the same reaction conditions except for the introduction of SYBR Green (Bio-Rad CFX Manager, CA, USA), and the relative expressions were calculated by the delta-delta comparative threshold (ΔΔ CT) method. Glyceraldehyde 3-phosphate dehydrogenase (GAPDH) served as an internal control.

Western Blot Analysis

After treatment with radioimmunoprecipitation assay (RIPA) buffer for 30 min, approximately 20 to 30 μg of cell lysates was used for western blot analysis, as previously reported.[48] Proteins were detected with the following antibodies: anti-LEF1 (1: 1,000; Cell Signaling Technology; C12A5), anti-c-Myc (1:1,000; Cell Signaling Technology; D84C12), anti-cyclin D1 (1: 1,000; Cell Signaling Technology; 92G2), anti-Bcl-2 (1:1,000; Abcam; ab692), anti-Bax (1:1,000; Santa Cruz Biotechnology; SC-493), and anti-β-actin (1:2,000; Santa Cruz Biotechnology; SC-32233).

Cell-Cycle Analysis

The cells in each group were collected after 48 h of transfection. After washing with cold PBS three times, the cell pellets were resuspended in PBS with the cell density of 1×10^5 cells/mL. After treatment with 400 μL of PI (Sigma-Aldrich, St. Louis, MO, USA), the samples were incubated for 30 min in the darkness at 4°C. The cell cycle was detected using red fluorescence with an automated fluorescence cell counter (Arthur; NanoEnTek, Seoul, Korea).

Flow Cytometry

After cell transfection, the cells in each group were digested with ethylene diamine tetraacetic acid (EDTA) and then collected in a flow tube. After 3 PBS washes, each sample was subjected to the Annexin-V fluorescein isothiocyanate (FITC) cell apoptosis kit (Sigma-Aldrich, St. Louis, MO, USA), following the kit instructions. The Annexin-V-FITC/PI dye was added to the 1×10^6 cell suspension. After a 15-min incubation at room temperature, the 525-nm and 620-nm band-pass filter was used for FITC and PI fluorescence detection, and the excitation wavelength of 488 nm was used for the detection of cell apoptosis.

Donor Construct Design and CRISPR/Cas9-Mediated Gene Editing

The transgene insertion system using CRISPR/Cas9 into the AAVS1 locus was derived from OriGene Technologies (https://www.origene.com/products/gene-expression/crispr-cas9) and consists of pCas-Guide-AAVS1 (#GE 100023) and pAAVS1-EF1a-Puro-DNR (#GE 100046). The donor vector contains 550 bp left, right homology arms matched to the AAVS1 locus in each side, followed by the

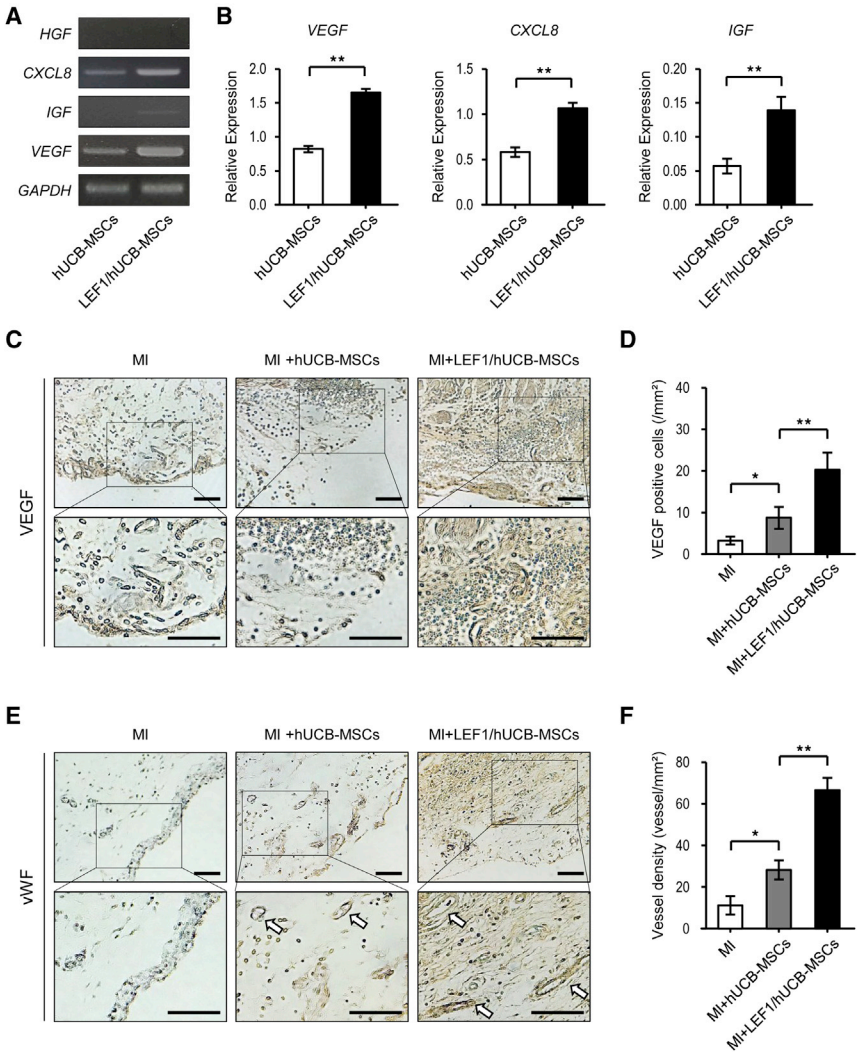

Figure 7. LEF1 Triggered Therapeutic Gene (VEGF, IL-8, IGF) Expressions and Enhanced Angiogenesis in MI + LEF1/hUCB-MSCs

(A) Expression of growth factors HGF, CXCL8, IGF, and VEGF was measured by conventional PCR. (B) Increased mRNA expression of growth factors in LEF1/hUCB-MSCs compared with hUCB-MSCs. Real-time PCR demonstrated that the relative gene expressions of VEGF, CXCL8, and IGF to GAPDH were increased in LEF1/hUCB-MSCs. **p < 0.01. (C) Immunohistochemical staining for VEGF in three MI groups: MI alone, MI + hUCB-MSCs, and LEF1/MI + hUCB-MSCs. Anti-VEGF antibody faintly stained rat heart, but a stronger signal was detected in LEF1/hUCB-MSCs. Scale bars, 100 μm. (D) VEGF protein expression was measured in infarcted heart among different groups (n = 5). (E) Immunohistochemical staining for vWF in three MI groups: MI alone, MI + hUCB-MSCs, and LEF1/MI + hUCB-MSCs. The blood vessels are stained in brown (arrows). More vessels were observed in MI + LEF1/hUCB-MSCs. Scale bars, 100 μm. (F) Higher vascular densities were detected in the MI + LEF1/hUCB-MSC group than in the MI-alone and MI + hUCB-MSC groups (n = 5). *p < 0.05 and **p < 0.01.

EF1α (EF1a) promoter for the constitutive expression of the target gene.

To insert the LEF1 gene in the donor vector, the LEF1 plasmid (#RC 208663) was purchased from OriGene (Rockville, MD, USA). The donor vector and LEF1 plasmid were digested with SgfI/MluI (NEB, Ipswich, MA, USA). This fragment was synthesized *de novo* and ligated into the donor vector to generate pAAVS1-EF1a-LEF1-DNR. To generate the LEF1/hUCB-MSCs, hUCB-MSCs were co-transfected with pCas-Guide-AAVS1 and pAAVS1-EF1a-LEF1-DNR through electroporation with the Neon Transfection System (Thermo Fisher Scientific).

MI Rat Model and Cell-Sheet Transplantation

The MI rat models were surgically induced, as previously described.[8] Briefly, male Sprague-Dawley rats, weighing 260–300 g (Orient Bio, Seongnam, Korea), were used as the MI model. All animal experiments were performed in accordance with the guidelines of the Institutional Animal Care and Use Committee (IACUC; SNU-190307-2; Seoul National University, Korea). The rats were divided into four groups: rats that received *LEF1*/hUCB-MSCs with MI, hUCB-MSCs with MI, non-treated with MI, and sham (no-MI), and each group consisted of at least 5 rats.

For the transplantation of stem cells, the UpCell system was employed (Thermo Fisher Scientific, Waltham, MA). Cell sheets of *LEF1*/hUCB-MSCs or hUCB-MSCs were detached from the plates by incubating at 20°C for 20 min. After transplantation, the supporting membrane was removed, and the cell sheets showed stable attachment. To prevent the rat's immune rejection of the human cells, all rats received cyclosporine, as previously described.[47]

Masson's Trichrome Staining and Histological Analysis

After extraction of all mice hearts, they were washed with PBS, fixed, embedded, and sectioned into 5 μm sections. Masson's trichrome staining was performed according to instructions of the trichrome stain kit (Sigma-Aldrich, St. Louis, MO, USA). The infarct size, fibrosis, and scar thickness were quantified with ImageJ software (NIH, Bethesda, MD, USA).

Immunohistochemical Staining

Immunohistochemical staining was performed using a standard protocol. The heart sections were incubated overnight with the following primary antibodies: anti-lamin A + C (1:200; Abcam; ab108922), anti-LEF1 (1:200; Cell Signaling Technology; C12A5), anti-VEGF (1:200;

Abcam; ab69479), and anti-vWF (1:200; Abcam; ab6994), and then they were subsequently exposed to biotinylated a secondary antibody and streptavidin peroxidase complex using the Histostain-Plus kit (Sigma-Aldrich, St. Louis, MO, USA). Then, the sections were stained with, 3′-diaminobenzidine tetra hydrochloride (Liquid DAB substrate kit; Abcam).

Functional Assessment of the Infarcted Myocardium

The measurement of cardiac function was performed, as previously reported.[8] Briefly, it was assessed by transthoracic echocardiography prior to MI surgery (normal baseline) and both 1 and 4 weeks after MI for every experimental group.

Statistical Analysis

Data are expressed as the mean ± SEM. For statistical analysis of multiple groups, 1-way ANOVA was performed, followed by a Bonferroni post hoc test. For verification of the therapeutic effects in MI, 2-way ANOVA was carried out, followed by a Bonferroni post hoc test. A p value less than 0.05 was considered statistically significant.

SUPPLEMENTAL INFORMATION

Supplemental Information can be found online at https://doi.org/10.1016/j.omtn.2020.01.007.

AUTHOR CONTRIBUTIONS

J.-Y.C. conceived and developed the entire study. H.-M.C. mainly analyzed data. K.-H.L. wrote the first draft of the manuscript. Y.-m.S. performed rat surgery for MI induction. T.-J.S. assisted all experiments. P.-D.R. supported scientific discussion. M.-C.C. performed echocardiography. K.-S.K. provided hUCB-MSCs. All of the authors discussed the results and contributed to the final manuscript.

CONFLICTS OF INTEREST

The authors declare no competing interests.

ACKNOWLEDGMENTS

All supporting materials were included in Supplemental Information. This research was supported by the Bio & Medical Technology Development Program of the National Research Foundation (NRF) of Korea, funded by the Ministry of Science and ICT (2016M3A9B6026771 and 2012M3A9C6049716).

REFERENCES

1. GBD 2016 Causes of Death Collaborators (2017). Global, regional, and national age-sex specific mortality for 264 causes of death, 1980–016: a systematic analysis for the Global Burden of Disease Study 2016. Lancet *390*, 1151–1210.
2. Jessup, M., and Brozena, S. (2003). Heart failure. N. Engl. J. Med. *348*, 2007–2018.
3. Neri, M., Riezzo, I., Pascale, N., Pomara, C., and Turillazzi, E. (2017). Ischemia/Reperfusion Injury following Acute Myocardial Infarction: A Critical Issue for Clinicians and Forensic Pathologists. Mediators Inflamm. *2017*, 7018393.
4. Nagamura-Inoue, T., and He, H. (2014). Umbilical cord-derived mesenchymal stem cells: Their advantages and potential clinical utility. World J. Stem Cells *6*, 195–202.
5. Amado, L.C., Saliaris, A.P., Schuleri, K.H., St John, M., Xie, J.S., Cattaneo, S., Durand, D.J., Fitton, T., Kuang, J.Q., Stewart, G., et al. (2005). Cardiac repair with intramyocardial injection of allogeneic mesenchymal stem cells after myocardial infarction. Proc. Natl. Acad. Sci. USA *102*, 11474–11479.
6. Tang, Y.L., Zhao, Q., Qin, X., Shen, L., Cheng, L., Ge, J., and Phillips, M.I. (2005). Paracrine action enhances the effects of autologous mesenchymal stem cell transplantation on vascular regeneration in rat model of myocardial infarction. Ann. Thorac. Surg. *80*, 229–236, discussion 236–237.
7. Cai, M., Shen, R., Song, L., Lu, M., Wang, J., Zhao, S., Tang, Y., Meng, X., Li, Z., and He, Z.X. (2016). Bone Marrow Mesenchymal Stem Cells (BM-MSCs) Improve Heart Function in Swine Myocardial Infarction Model through Paracrine Effects. Sci. Rep. *6*, 28250.
8. Cho, H.M., Kim, P.H., Chang, H.K., Shen, Y.M., Bonsra, K., Kang, B.J., Yum, S.Y., Kim, J.H., Lee, S.Y., Choi, M.C., et al. (2017). Targeted Genome Engineering to Control VEGF Expression in Human Umbilical Cord Blood-Derived Mesenchymal Stem Cells: Potential Implications for the Treatment of Myocardial Infarction. Stem Cells Transl. Med. *6*, 1040–1051.
9. Ferrara, N., Gerber, H.P., and LeCouter, J. (2003). The biology of VEGF and its receptors. Nat. Med. *9*, 669–676.
10. Xiang, Q., Liao, Y., Chao, H., Huang, W., Liu, J., Chen, H., Hong, D., Zou, Z., Xiang, A.P., and Li, W. (2018). ISL1 overexpression enhances the survival of transplanted human mesenchymal stem cells in a murine myocardial infarction model. Stem Cell Res. Ther. *9*, 51.
11. Zhao, L., Liu, X., Zhang, Y., Liang, X., Ding, Y., Xu, Y., Fang, Z., and Zhang, F. (2016). Enhanced cell survival and paracrine effects of mesenchymal stem cells overexpressing hepatocyte growth factor promote cardioprotection in myocardial infarction. Exp. Cell Res. *344*, 30–39.
12. Li, J., Li, J., and Chen, B. (2012). Oct4 was a novel target of Wnt signaling pathway. Mol. Cell. Biochem. *362*, 233–240.
13. Huang, C., and Qin, D. (2010). Role of Lef1 in sustaining self-renewal in mouse embryonic stem cells. J. Genet. Genomics *37*, 441–449.
14. Kim, C.G., Chung, I.Y., Lim, Y., Lee, Y.H., and Shin, S.Y. (2011). A Tcf/Lef element within the enhancer region of the human NANOG gene plays a role in promoter activation. Biochem. Biophys. Res. Commun. *410*, 637–642.
15. Okamura, R.M., Sigvardsson, M., Galceran, J., Verbeek, S., Clevers, H., and Grosschedl, R. (1998). Redundant regulation of T cell differentiation and TCRalpha gene expression by the transcription factors LEF-1 and TCF-1. Immunity *8*, 11–20.
16. Staal, F.J., Luis, T.C., and Tiemessen, M.M. (2008). WNT signalling in the immune system: WNT is spreading its wings. Nat. Rev. Immunol. *8*, 581–593.
17. Armenteros, T., Andreu, Z., Hortigüela, R., Lie, D.C., and Mira, H. (2018). BMP and WNT signalling cooperate through LEF1 in the neuronal specification of adult hippocampal neural stem and progenitor cells. Sci. Rep. *8*, 9241.
18. Zhang, Y., Yu, J., Shi, C., Huang, Y., Wang, Y., Yang, T., and Yang, J. (2013). Lef1 contributes to the differentiation of bulge stem cells by nuclear translocation and crosstalk with the Notch signaling pathway. Int. J. Med. Sci. *10*, 738–746.
19. Li, Y., Lin, B., and Yang, L. (2015). Comparative transcriptomic analysis of multiple cardiovascular fates from embryonic stem cells predicts novel regulators in human cardiogenesis. Sci. Rep. *5*, 9758.
20. Liu, Q., Jiang, C., Xu, J., Zhao, M.T., Van Bortle, K., Cheng, X., Wang, G., Chang, H.Y., Wu, J.C., and Snyder, M.P. (2017). Genome-Wide Temporal Profiling of Transcriptome and Open Chromatin of Early Cardiomyocyte Differentiation Derived From hiPSCs and hESCs. Circ. Res. *121*, 376–391.
21. Ye, B., Li, L., Xu, H., Chen, Y., and Li, F. (2019). Opposing roles of TCF7/LEF1 and TCF7L2 in cyclin D2 and Bmp4 expression and cardiomyocyte cell cycle control during late heart development. Lab. Invest. *99*, 807–818.
22. Gaj, T., Gersbach, C.A., and Barbas, C.F., 3rd (2013). ZFN, TALEN, and CRISPR/Cas-based methods for genome engineering. Trends Biotechnol. *31*, 397–405.
23. Carroll, D. (2011). Genome engineering with zinc-finger nucleases. Genetics *188*, 773–782.
24. Joung, J.K., and Sander, J.D. (2013). TALENs: a widely applicable technology for targeted genome editing. Nat. Rev. Mol. Cell Biol. *14*, 49–55.

25. Cong, L., Ran, F.A., Cox, D., Lin, S., Barretto, R., Habib, N., Hsu, P.D., Wu, X., Jiang, W., Marraffini, L.A., and Zhang, F. (2013). Multiplex genome engineering using CRISPR/Cas systems. Science *339*, 819–823.

26. Hsu, P.D., Lander, E.S., and Zhang, F. (2014). Development and applications of CRISPR-Cas9 for genome engineering. Cell *157*, 1262–1278.

27. Sander, J.D., and Joung, J.K. (2014). CRISPR-Cas systems for editing, regulating and targeting genomes. Nat. Biotechnol. *32*, 347–355.

28. de la Fuente-Núñez, C., and Lu, T.K. (2017). CRISPR-Cas9 technology: applications in genome engineering, development of sequence-specific antimicrobials, and future prospects. Integr. Biol. *9*, 109–122.

29. Tateno, H., Hiemori, K., Hirayasu, K., Sougawa, N., Fukuda, M., Warashina, M., Amano, M., Funakoshi, T., Sadamura, Y., Miyagawa, S., et al. (2017). Development of a practical sandwich assay to detect human pluripotent stem cells using cell culture media. Regen Ther *6*, 1–8.

30. Lian, X., Hsiao, C., Wilson, G., Zhu, K., Hazeltine, L.B., Azarin, S.M., Raval, K.K., Zhang, J., Kamp, T.J., and Palecek, S.P. (2012). Robust cardiomyocyte differentiation from human pluripotent stem cells via temporal modulation of canonical Wnt signaling. Proc. Natl. Acad. Sci. USA *109*, E1848–E1857.

31. Witman, N., and Sahara, M. (2018). Cardiac Progenitor Cells in Basic Biology and Regenerative Medicine. Stem Cells Int. *2018*, 8283648.

32. Reya, T., O'Riordan, M., Okamura, R., Devaney, E., Willert, K., Nusse, R., and Grosschedl, R. (2000). Wnt signaling regulates B lymphocyte proliferation through a LEF-1 dependent mechanism. Immunity *13*, 15–24.

33. Segers, V.F., and Lee, R.T. (2008). Stem-cell therapy for cardiac disease. Nature *451*, 937–942.

34. Toma, C., Pittenger, M.F., Cahill, K.S., Byrne, B.J., and Kessler, P.D. (2002). Human mesenchymal stem cells differentiate to a cardiomyocyte phenotype in the adult murine heart. Circulation *105*, 93–98.

35. Tompkins, B.A., Natsumeda, M., Balkan, W., and Hare, J.M. (2017). What Is the Future of Cell-Based Therapy for Acute Myocardial Infarction. Circ. Res. *120*, 252–255.

36. Enoki, C., Otani, H., Sato, D., Okada, T., Hattori, R., and Imamura, H. (2010). Enhanced mesenchymal cell engraftment by IGF-1 improves left ventricular function in rats undergoing myocardial infarction. Int. J. Cardiol. *138*, 9–18.

37. Chang, H.K., Kim, P.H., Kim, D.W., Cho, H.M., Jeong, M.J., Kim, D.H., Joung, Y.K., Lim, K.S., Kim, H.B., Lim, H.C., et al. (2018). Coronary stents with inducible VEGF/HGF-secreting UCB-MSCs reduced restenosis and increased re-endothelialization in a swine model. Exp. Mol. Med. *50*, 114.

38. Pannitteri, G., Marino, B., Campa, P.P., Martucci, R., Testa, U., and Peschle, C. (1997). Interleukins 6 and 8 as mediators of acute phase response in acute myocardial infarction. Am. J. Cardiol. *80*, 622–625.

39. Lee, C.Y., Kim, R., Ham, O., Lee, J., Kim, P., Lee, S., Oh, S., Lee, H., Lee, M., Kim, J., and Chang, W. (2016). Therapeutic Potential of Stem Cells Strategy for Cardiovascular Diseases. Stem Cells Int. *2016*, 4285938.

40. Aloysius, A., DasGupta, R., and Dhawan, J. (2018). The transcription factor Lef1 switches partners from β-catenin to Smad3 during muscle stem cell quiescence. Sci. Signal. *11*, eaan3000.

41. Denu, R.A., and Hematti, P. (2016). Effects of Oxidative Stress on Mesenchymal Stem Cell Biology. Oxid. Med. Cell. Longev. *2016*, 2989076.

42. Kim, K., Pang, K.M., Evans, M., and Hay, E.D. (2000). Overexpression of beta-catenin induces apoptosis independent of its transactivation function with LEF-1 or the involvement of major G1 cell cycle regulators. Mol. Biol. Cell *11*, 3509–3523.

43. Zhao, Y., Li, C., Huang, L., Niu, S., Lu, Q., Gong, D., Huang, S., Yuan, Y., and Chen, H. (2018). Prognostic value of association of OCT4 with LEF1 expression in esophageal squamous cell carcinoma and their impact on epithelial-mesenchymal transition, invasion, and migration. Cancer Med. *7*, 3977–3987.

44. Lamb, R., Ablett, M.P., Spence, K., Landberg, G., Sims, A.H., and Clarke, R.B. (2013). Wnt pathway activity in breast cancer sub-types and stem-like cells. PLoS ONE *8*, e67811.

45. Shtutman, M., Zhurinsky, J., Simcha, I., Albanese, C., D'Amico, M., Pestell, R., and Ben-Ze'ev, A. (1999). The cyclin D1 gene is a target of the beta-catenin/LEF-1 pathway. Proc. Natl. Acad. Sci. USA *96*, 5522–5527.

46. Espada, J., Calvo, M.B., Díaz-Prado, S., and Medina, V. (2009). Wnt signalling and cancer stem cells. Clin. Transl. Oncol. *11*, 411–427.

47. Kang, B.J., Kim, H., Lee, S.K., Kim, J., Shen, Y., Jung, S., Kang, K.S., Im, S.G., Lee, S.Y., Choi, M., et al. (2014). Umbilical-cord-blood-derived mesenchymal stem cells seeded onto fibronectin-immobilized polycaprolactone nanofiber improve cardiac function. Acta Biomater. *10*, 3007–3017.

48. Lee, J.H., Kim, B.G., Ahn, J.M., Park, H.J., Park, S.K., Yoo, J.S., Yates, J.R., 3rd, and Cho, J.Y. (2010). Role of PI3K on the regulation of BMP2-induced beta-Catenin activation in human bone marrow stem cells. Bone *46*, 1522–1532.

OMTN, Volume *19*

Supplemental Information

Transplantation of hMSCs Genome Edited with LEF1 Improves Cardio-Protective Effects in Myocardial Infarction

Hyun-Min Cho, Kang-Hoon Lee, Yi-ming Shen, Tae-Jin Shin, Pan-Dong Ryu, Min-Cheol Choi, Kyung-Sun Kang, and Je-Yoel Cho

Supplemental Table 1. Top 100 up-regulated genes in mesoderm, cardiac mesoderm and cardiac progenitor cells from 8 different transcriptome analysis.

Feng Cao et al. 2008

Beating EB/hESCs

Gene Symbol	Fold Change
MYOZ2	250.1
TBX5	222.6
SRD5A2L2	206.7
HOXA3	197.6
ALB	191.9
CFI	173
PLN	127.2
SKIP	107.8
EDN3	99.9
MYH6	96.9
BNC1	92.7
SMPX	87.4
C5orf23	80
TM4SF4	77.4
HOXB3	73
NTRK2	70.2
PRND	64.7
ALDH1A2	61.3
EBF3	61.2
EPHA3	59.4
MEIS2	54.6
LIPC	53.9
FOXC1	52
EBF3	50.7
CNTNAP4	50.2
TBX2	45.7
SCRG1	45.6
KBTBD10	44.7
PLN	44.4
VCAM1	42
EYA4	41.5
COL3A1	38.2
FOXF2	37.2
NELL1	36.9

* hESCs, human embryonic stem cells

CR615016	36.1
KIAA1713	36.1
ISL1	35.6
AMBP	34.7
PHOX2B	34.1
EVI1	32.9
RP11-301I17.1	32.7
CNTN4	32
POPDC2	32
LOC399959	31.4
GDF6	31.3
DACH1	30.5
ITIH2	29.7
ACTN2	29.3
MEIS2	28.7
MEF2C	28.4
AK021804	28
SULT1E1	27.1
EBF3	26.4
SLC8A3	26.3
NR2F2	26.2
PLAGL1	26.2
HOXB4	26.1
TNNT2	26.1
ZIC1	25.8
MYLPF	25.2
PDE11A	24.8
RASGRP3	24.5
MYL7	23.9
AGT	23.9
GPC5	23.7
TRH	23.7
RARB	23.6
MEIS1	23.3
DYNLRB2	23.3
TWIST1	22.4
RFTN2	22.4
POSTN	21.9
PPP1R14C	21.7
PDZRN4	21.6
AHSG	21.3
SYNPO2	21.3
APOB	21.2

ZNF25	21.1
LIX1	20.5
COL3A1	20.3
ITIH5	20.2
SMOC2	19.7
BMP4	19.5
FGG	19.2
OSR2	19
MYL4	18.9
THC2672869	18.9
SCD5	18.7
TGFB3	18.4
MBD2	18.3
SNAI2	18.3
EYA1	17.9
TSHZ2	17.8
A2M	17.7
APOB	17.4
FOXA1	17.3
FLRT2	17.3
MSX2	17.2
SCML1	16.6
GATA5	16.3

Yang Li et al. 2015

MCP/hES

Gene Symbol	Fold Change
FOSB	490.2042
FOS	452.1115
NR_002835	115.5838
HAND1	94.48368
EGR1	80.32818
DKK1	76.05242
MEIS1	62.6408
LIX1	58.27843
LEF1	58.03548
JUN	57.208
DNAH2	55.96155
GATA6	50.23384
MSX1	48.69569
SNAI2	42.64225
NR4A1	40.6673
MEIS2	36.13636
HOXB2	32.50254
MLC2a	32.2342
HOXB3	30.40221
GATA4	30.03541
BMP5	21.65403
IRX3	19.54113
SFRP5	19.51239
JUNB	18.73348
EPHB2	18.64964
EPHB3	18.40125
KLF6	18.0868
EPHA4	16.46524
EGR3	14.72606
BTRC	14.05589
AMHR2	13.77047
SMAD6	13.27864
NKX2-5	12.63155
HES1	12.59014
EGR2	11.71461
HAND2	11.59452
FZD2	11.39963

* MCP, multipotential cardiovascular progenitors
* hES, human embryonic stem cells

TBX3	10.97677
TBX20	10.79458
EFNA1	10.39215
LHX1	10.32808
BMP4	10.24145
WNT9B	9.867736
BMP2	9.68734
TMEM185A	9.680868
SP6	9.597183
JUND	9.58426
ISL1	8.878495
HEY1	8.692293
WNT5A	8.255593
SP5	7.928157
NKX3-1	7.903193
CHRD	7.84345
WNT3	7.773142
RGS5	7.727929
MICAL2	7.63259
THBS1	7.548299
MYOCD	7.356116
NR_033947	7.309524
NKD1	7.071277
NR_028342	7.05
LRRTM1	6.826144
HOXB1	6.659542
EFNB3	6.512254
IRX5	6.492784
KLF1	6.342381
MAPK10	6.248503
PROX1	6.232521
SETBP1	6.196129
NR_003697	6.17
PLAGL1	6.003675
NR_002729	5.632479
SIX1	5.61734
NFATC1	5.38123
FZD4	5.331868
TBX2	5.278557
EFNB2	5.211594
SMAD7	5.057645
SALL1	5.042952
SHC2	4.515965

ATF3	4.503114
NR_034035	4.35
JAG1	4.346944
CRIP1	4.317952
PITX1	4.242204
EPHB6	4.182669
NR_024593	3.75
LBH	3.748008
TGFB2	3.730964
SCMH1	3.723372
THBS3	3.599518
ZNF703	3.587365
NR_022014	3.526936
SOX18	3.502705
SRC	3.467945
HOXB5	3.461189
MAML3	3.322157
EVX1	3.22485
CBLB	3.217233
DLL3	3.206268

Miao Zhang et al. 2015 (2D)

Cardiac precursor stage (1 Week)/hES

Gene Symbol	Fold Change
MYH6	3979.586
MYL4	2526.432
VCAM1	1024.034
SMPX	1007.62
MYOM1	941.3134
ALPK2	927.4772
HAND1	875.2244
TNNT2	843.0856
MYBPC3	810.8523
HSPB7	657.1956
NKX2-5	634.279
CKM	624.2534
SORBS2	621.586
SORBS2	574.2605
MYL3	553.1304
TNNT2	530.988
TCEA3	505.456
MASP1	492.9746
RSPO3	379.7014
WNT2	375.918
SRD5A2L2	364.49
TRIM55	311.7068
ADPRHL1	309.8999
PGM5	302.599
BMP5	295.4562
MASP1	295.0512
TBX2	290.3812
SMYD1	289.9152
PGM5	289.1124
FHOD3	287.1828
PLN	272.0014
CSHL1	262.2302
MYL7	258.7866
TMOD1	247.9816
COL3A1	244.4418
MEIS2	242.6402
TNNC1	236.453

* hES, human embryonic stem cells

APOBEC2	229.8642
ACTC1	226.5503
POPDC2	222.6694
MASP1	222.0394
SMPX	219.3103
SYNPO2L	206.8522
MB	196.8003
RBM24	186.2591
MYH7	174.9472
VCAM1	173.6631
SGPP2	157.5902
ACTN2	153.3807
HSPB2	147.7327
TGM2	144.5446
TRIM55	140.4074
XIRP1	128.1629
CRYAB	126.8296
NPPA	126.2408
GUCY1A3	125.6104
IRX3	124.4145
ACTA2	119.0433
FBXO32	116.9635
UNC45B	115.7094
RRAD	115.0351
ZNF503	113.3776
PPP1R14C	111.6746
H2AFY	111.5748
MYLK3	109.1334
ZNF503	108.787
H19	106.8246
LIX1	105.5454
S1PR1	103.2021
RBM24	102.5497
CSRP3	100.3465
CACNA1C	99.87034
FGF18	98.87316
MB	98.44745
CCDC141	93.98728
ZEB2	93.48793
KIF26B	93.42158
FHL2	92.48632
ENO3	90.39511
HAPLN1	88.13806

LOC441081	86.92248
NID2	85.72912
PGM5	85.46334
DOK4	82.6236
CORIN	81.10888
LAMA4	80.50386
SRL	80.42206
RBM20	80.2577
GATA5	77.913
FIT1	77.05922
REEP1	74.05532
HAPLN1	73.85769
SLIT3	73.06123
C1orf117	72.17776
RRAD	71.34848
MSX2	70.87422
EDG1	70.62046
IRX5	67.68796
RGS5	67.53217
TRIM63	66.16686

Miao Zhang et al. 2015 (3D)

Cardiac precursor stage (1 Week)/hES

Gene Symbol	Fold Change
MYH6	399.3081
MYL4	167.6815
TNNT2	139.5036
SMPX	134.139
TNNT2	118.261
VCAM1	98.22121
ALPK2	88.81647
MYL7	86.37505
TNNC1	81.00194
MYBPC3	77.95404
SORBS2	76.97758
HSPB7	63.54108
ADPRHL1	55.20673
ENO3	53.38229
ACTC1	52.18965
CKM	51.32686
MYOM1	49.10574
TCEA3	43.53546
NKX2-5	42.23927
ACTA2	41.91131
PLN	41.45757
WNT2	41.35147
SORBS2	40.1369
COL3A1	39.58095
HAND1	39.06372
MYL3	39.02715
DOK4	37.08353
IRX3	36.32548
TMOD1	35.65121
BMP4	31.72424
PGM5	29.45128
VCAM1	29.2067
NEBL	29.18869
CRIP1	28.82436
RSPO3	28.60389
MASP1	28.59886
MASP1	28.17681

* hES, human embryonic stem cells

COL22A1	27.62911
PGM5	27.1114
SMPX	26.83504
KCTD12	26.18157
RBM24	26.14811
FHOD3	26.04482
TNFRSF19	25.45603
TBX2	25.39101
H19	25.33552
ENO3	24.85976
SMYD1	24.3245
GPR177	24.00319
SRD5A2L2	23.37857
ACTN2	22.84624
NID2	22.80724
NEXN	22.38514
MASP1	22.06302
NDRG2	21.27696
TGFBI	20.30832
H2AFY	19.96608
CRIP2	19.43907
TRIM55	18.99967
MEIS2	18.42141
GJA3	18.28533
MB	17.88436
PKP2	17.64615
LAMA4	17.48894
SLIT3	17.20535
MYH7	17.18687
FBXO32	17.08549
KLHL14	16.74788
FLNC	16.46425
CSHL1	16.05042
LEF1	16.02262
PGM5	15.83551
FGF18	15.83224
PKIA	15.81365
SGPP2	15.24684
APOBEC2	15.24054
PALLD	14.94056
RIN2	14.75904
PPP1R3C	14.42754
SIRPA	14.29529

CCDC141	14.04552
SYNPO2L	13.83302
LIX1	13.75648
SLC30A3	13.69237
POPDC2	13.64602
BVES	13.4341
HAPLN1	13.38557
PTH1R	13.38018
MYLK3	13.26614
PPP1R14C	13.19338
SH3PXD2A	13.16491
MYL9	13.11668
FBN2	13.11462
CAP2	13.0534
CCDC80	12.84676
S1PR1	12.79504
MB	12.78877
HSPB2	12.72478
HRC	12.6484
MSRB3	12.57696

Qing Liu et al. 2017 (hESCs)

Mesoderm (day 2)/hES

Gene Symbol	Fold Change
HOXB1	7130.484
HOXA3	2575.088
WNT8A	504.5474
BC047600	479.9686
LINC00261	433.1659
ZEB2	425.8732
HOXB9	401.6111
HOXB3	329.7081
LINC00113	276.1072
APLNR	242.2131
TBX3	215.5371
PCAT1	168.604
LOC100506178	158.8516
LOC100130480	153.8936
AK094352	132.3637
LEF1	105.1897
SLC8A3	98.41792
FOXC1	80.37095
UBE2DNL	78.91943
LINC00314	77.42062
SEZ6L	75.483
WLS	66.74832
SLIT2-IT1	58.75452
ZEB2-AS1	57.88815
DIO3AS	57.03059
LGR5	53.54275
CNTFR	51.68412
ALG1L2	45.95042
TMEM132C	44.65068
OR5AK4P	43.21352
LIX1	41.09082
GREB1L	35.69386
HHIPL2	35.18348
MCOLN3	33.98602
AX747586	32.35689
BC038746	30.47513
ANKRD55	28.52414

* hES, human embryonic stem cells

NR0B1	24.83537
AK311342	22.47887
PLXNA2	21.96499
CER1	21.29729
BC042046	21.05146
WNT3	20.39505
WDR93	19.70002
DQ601842	19.64008
LINC00645	17.88646
CDH11	17.87995
BAHCC1	17.75231
LOC729732	17.64674
SNAI2	17.58228
FOXF1	17.51243
CYP1B1-AS1	17.26308
MIR5583-1	16.85834
LOC100507266	16.7959
PRTG	16.6573
AK095285	16.5344
DIO3	16.51031
FSHR	16.2586
MIR5695	16.20566
LOC100505918	16.14733
COL13A1	16.00323
AK091996	15.97935
CXCR4	15.82085
GLRA4	15.82063
PRUNE2	15.59235
OMD	15.19963
BC040863	15.04204
DQ570035	14.71315
TAS2R4	14.44581
HS3ST1	14.36105
RPA4	14.3032
OR10A4	14.25488
MIR4529	14.09601
SPON1	14.09528
CYP1B1	13.89062
TNC	13.84048
TMEM119	13.70854
AK125301	13.58132
MEPE	13.23464
DQ576445	13.15407

BX537950	12.90041
LGALS12	12.72606
HAS2	12.36848
HAS2-AS1	12.36587
ANGPT2	12.09688
MESP1	11.81933
PRSS37	11.79572
MIR181A2HG	11.67688
OR10A2	11.53347
BC040861	11.39477
ARSD	11.15455
EPHA4	11.11665
NRXN3	11.11621
UNC5C	11.10834
MSX2	10.91508
GPR83	10.82935
ROR2	10.75628
BMPER	10.69815
TACR3	10.6596
ITGA8	10.48024

Qing Liu et al. 2017 (hESCs)

Cardiac mesoderm (day 4)/hES	
Gene Symbol	Fold Change
HOXB1	5607.15
ITGA8	1870.598
HOXA3	1210.592
LIX1	1096.973
HOXB9	952.7214
LINC00261	895.0882
TBX3	803.4978
APLNR	688.1215
ZAP70	673.3462
ZEB2	576.6249
HOXB3	489.5344
WNT8A	423.2092
LGR5	419.1213
PLXNA4	324.4826
GREB1L	310.6925
LOC100130480	310.2802
OR5AK4P	250.8534
UBE2DNL	246.4806
SOX1	209.592
BC047600	188.9781
HHIPL2	183.8207
BMPER	182.1447
HOXB-AS3	178.7448
OLIG3	177.8665
LHX1	160.849
AK094352	157.8193
WDR93	146.9692
MSX2	139.5033
FSHR	138.2824
HAS2	138.0719
DRD2	134.8252
NRG2	132.2017
ZEB2-AS1	128.7818
AMER3	127.9505
LRRTM1	125.0852
LOC100506178	122.4121
LGALS12	121.6388

* hES, human embryonic stem cells

LEF1	117.1546
TMEM132C	116.1481
LINC00113	111.8552
FOXC1	108.5072
HAS2-AS1	104.6359
HLX	99.66891
WNT1	93.60181
PLXNA2	81.62751
BC048130	80.29126
WLS	78.90398
BC038746	76.79686
SNAI2	75.62271
ANKRD55	74.94878
FOXF1	74.63355
BC153822	67.03655
CDH11	64.04853
MCOLN3	62.12916
DIO3AS	60.00674
SEZ6L	56.34601
GLRA4	55.06328
KCNA1	54.84662
SLIT2-IT1	51.79549
PCAT1	51.71063
PRTG	51.0873
NTRK1	51.01311
AX748340	50.71157
SLC8A3	49.10156
MESP1	47.86788
CNTFR	47.5286
BMP4	41.74337
LINC00922	41.61498
CXCR4	38.55703
SMOC1	37.0814
ANGPT2	36.65889
LINC00314	36.22408
PCDH8	35.75861
TNC	33.62822
PLEKHA6	31.85229
TMEM88	30.59094
COLEC12	30.50178
KIAA1462	29.28957
SAMD3	28.39264
LOC100996291	28.36061

COL13A1	27.91
BC084573	27.46686
KEL	27.43305
SPON1	26.39435
BAHCC1	26.35288
CDH22	24.99021
DIO3	24.72618
POTEC	24.01316
AMIGO2	22.72428
PRSS37	21.97482
DSCAM	21.82124
LINC00645	21.80164
ALG1L2	21.74399
CRB2	21.44234
PSKH2	21.19242
NPY	20.67031
MIR5695	20.64279
MESP2	19.19838
ST8SIA1	19.17423
TMEM190	19.13664

Qing Liu et al. 2017 (hiPSCs)

Mesoderm (day 2)/hiPSCs

Gene Symbol	Fold Change
WNT8A	7573.874
APLNR	1478.937
LEF1-AS1	612.725
ZEB2	567.6549
FSHR	560.9239
HOXA3	559.1082
LINC00314	509.4223
LIX1	389.6455
ANKRD55	377.4863
HOXA2	271.0282
OR5AK4P	241.3719
LINC00113	222.9561
LEF1	189.1034
SLC2A5	129.4292
BC048130	128.7367
CXCR4	118.0734
HHIPL2	114.2601
DIO3AS	110.8081
LHX1	108.7782
PCAT1	94.07109
FOXF1	86.98869
DIO3	78.16554
SLC8A3	73.54733
LINC00261	70.06185
PCDH8	66.87678
GREB1L	64.67749
COLEC12	62.11863
POTEC	60.68643
LRRC55	60.35236
LINC00479	59.53359
SNAI2	58.35102
BC047600	57.06436
NR0B1	55.88631
TMEM119	55.84367
UNC5C	55.36579
HOXB7	54.8008
WDR93	51.88953

* hiPSCs, human induced pluripotent stem cells

TBX3	50.84114
LGR5	48.03701
PLXNA2	47.06145
CDH11	46.1663
SEZ6L	45.26747
SLIT2-IT1	44.99943
HOXB3	41.59304
WLS	38.39509
LOC100507266	37.02074
LIN7A	36.20756
HOXB1	35.37803
PRTG	35.1072
LOC100506178	30.27245
AX748340	29.74274
BC029835	28.64437
JA611294	27.56238
TPH1	26.62607
HOXB9	26.51223
MSX2	24.62081
CER1	24.42643
ITGA8	23.95757
MCOLN3	23.57093
BMPER	22.90114
BMP2	22.71108
HLX	20.6525
PSKH2	19.96273
TMEM132C	19.67268
C8orf31	19.61278
BMP4	18.869
LOC100130480	18.78973
DQ601842	17.74326
BC038746	17.31094
MIR4529	16.99094
PCDH19	16.75686
EPHA4	16.2812
CA2	15.85538
COL13A1	15.74502
NPY	15.71137
DGKG	14.99456
ANPEP	14.69478
HAS2	14.56081
PDZK1	14.50893
MIR5695	13.4215

DNAH9	13.36378
LINC00941	13.33775
ST8SIA1	12.83828
LRRTM1	12.79385
HAS2-AS1	12.66779
TGFB1	12.38839
GPR83	11.72504
MAPK10	11.65603
SOAT1	11.32484
PKNOX2	11.20868
TNC	11.09238
BC046497	10.8955
BX537950	10.79865
BC040327	10.65811
BC043519	10.64531
FOXC1	10.55505
DSCAM	10.29913
ADAM20P1	10.23917
AX747586	10.17231
GLRA4	10.13699

Qing Liu et al. 2017 (hiPSCs)

Cardiac mesoderm (day 4)/hiPSCs

Gene Symbol	Fold Change
WNT8A	6408.818
ITGA8	2375.721
HLX	1478.267
APLNR	1397.819
FSHR	1162.332
LIX1	1045.706
OR5AK4P	765.4834
LINC00314	549.7784
LINC00261	542.7969
ZEB2	489.8526
BC029835	476.2523
LHX1	449.4342
LEF1-AS1	358.9401
BC048130	349.4714
NRG2	346.4435
GYPE	334.4045
PLXNA4	286.5325
GREB1L	281.796
LOC100130480	260.1327
BMPER	247.8012
LINC00113	246.2482
ANKRD55	240.0616
HOXA2	229.4163
AX748340	224.0679
POTEC	210.8303
HHIPL2	206.9498
BC047600	202.2095
AMER3	195.9735
LEF1	178.479
HOXA3	152.5046
WDR93	149.5502
MSX2	139.2078
LOC100506178	122.6939
PCDH8	119.4055
PCAT1	118.9039
LGR5	117.3004
HOXB5	113.0237

* hiPSCs, human induced pluripotent stem cells

HOXB7	112.116
NR0B1	108.781
SNAI2	99.95962
BMP4	99.08312
TNC	96.63648
PRTG	94.70793
SOX1	94.25291
KEL	93.42265
ST8SIA1	92.14639
HOXB9	90.10871
LRRTM1	87.25986
HAS2	87.22561
NTRK1	86.84461
LOC100996291	83.79417
PSKH2	80.27596
TMEM119	79.17451
NPY	75.21803
KCNA1	72.04527
LRRC55	68.95987
CDH22	68.79358
LIN7A	67.38447
DRD2	65.45551
ATP8B4	64.39406
CXCR4	63.93349
BMP2	63.91353
HAS2-AS1	62.6692
SAMD3	62.19359
BC153822	61.17402
TMEM88	60.20352
CDH11	60.02746
SLC2A5	58.91697
DIO3AS	57.9588
WLS	53.27906
HOXB3	50.36926
C8orf31	49.50918
FOXF1	49.06348
LINC00479	48.05903
BC038746	48.00503
DIO3	47.54033
UNC5C	47.07868
PLXNA2	46.58478
TMEM132C	45.29767
CRB2	44.26131

SLIT2-IT1	44.18941
KIAA1462	43.96861
COLEC12	43.12444
MESP2	42.74193
MCOLN3	40.23859
PGA5	39.8949
SLC8A3	39.80684
SMOC1	39.45719
PLEKHA6	39.20725
CER1	39.19738
BC084573	38.25622
GLRA4	35.77824
DSCAM	31.97191
TBX3	29.17848
CYP26A1	26.93133
LINC00922	26.17271
AK094352	25.15566
LGALS12	24.85304
GPR83	24.78127
NRG1	24.75436

Supplemental Figure. 1

A

GENE SYMBOL	ENSEMBL GENE ID	GENE NAME
LIX1	ENSG00000145721	Limb and CNS expressed 1
HOXB3	ENSG00000120093	Homeobox B3
LEF1	ENSG00000138795	Lymphoid enhancer binding factor 1
SNAI2	ENSG00000019549	Snail family transcriptional repressor 2
BMP4	ENSG00000125378	Bone morphogenetic protein 4
BMPER	ENSG00000164619	BMP binding endothelial regulator
MSX2	ENSG00000120149	Msh homeobox 2
PLXNA2	ENSG00000076356	Plexin A2
SLC8A3	ENSG00000100678	Solute carrier family 8 member A3
TBX3	ENSG00000135111	T-Box 3
ZEB2	ENSG00000169554	Zinc finger E-box binding homeobox 2

B

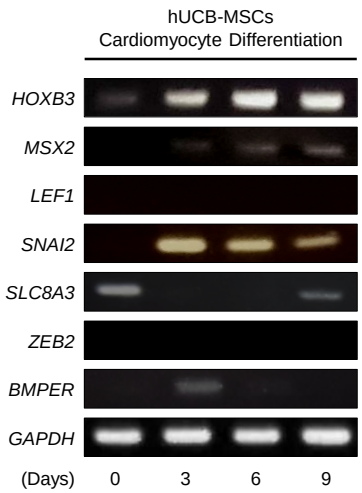

Supplemental Figure 1. List of genes selected from the in silico research and conventional PCR analysis of 7 target genes. (A) 11 genes commonly enriched in the stages from mesoderm to cardiac progenitor cells in more than 5 analysis. (B) Conventional PCR data of 7 target genes during cardiomyocyte differentiation of hUCB-MSCs.

Supplemental Figure. 2

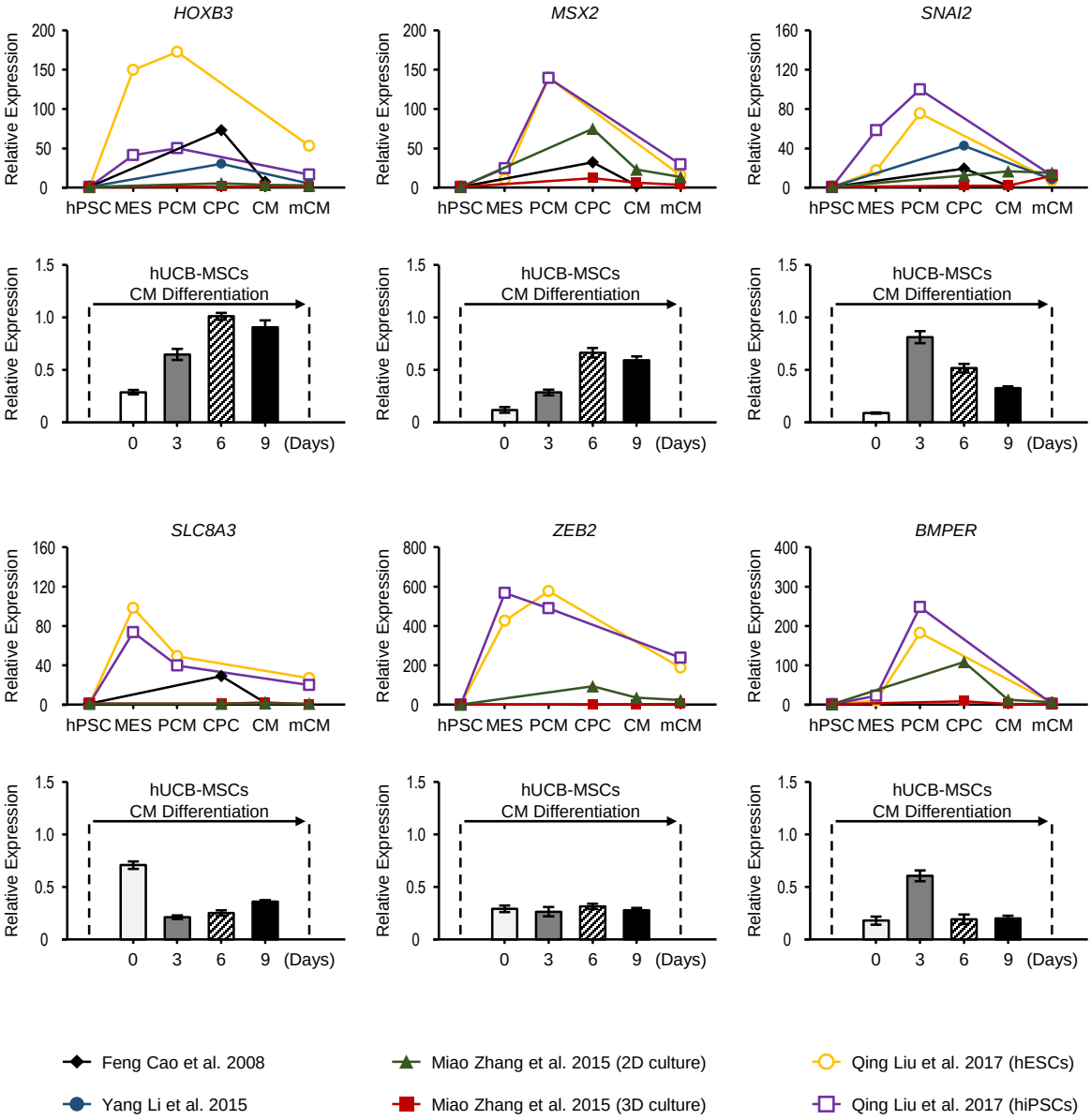

Supplemental Figure 2. Comparison of 6 genes expression between in silico literature surveys and qRT-PCR data. Except LEF1, the expression profiles of six target genes in CM differentiation were depicted with GAPDH, internal control gene expression.